Supporting Information Appendix

The Atg2-Atg18 complex tethers pre-autophagosomal membranes to the endoplasmic reticulum for autophagosome formation

Tetsuya Kotani[a], Hiromi Kirisako[a], Michiko Koizumi[b], Yoshinori Ohsumi[b], and Hitoshi Nakatogawa[a]

[a]School of Life Science and Technology, Tokyo Institute of Technology

[b]Institute of Innovative Research, Tokyo Institute of Technology

www.pnas.org/cgi/doi/10.1073/pnas.1806727115

SI Materials and Methods

Yeast Strains

Gene deletion and tagging of epitopes or fluorescent proteins were performed by a PCR-based method (1). To construct the strains used in Figs. 1B, 2C, 3B, pRS303-based plasmids were linearized with *Bsm*I prior to introduction into yeast cells. For construction of the strains used in Fig. 3C, pRS303- and pRS304-based plasmids were linearized with *Nhe1* and *Eco*RV, respectively.

Plasmids

The plasmids used in this study are listed in Table S2. Plasmids for the expression of Atg2-3×HA-EGFP were derived from pRS303 or pRS316 (2), and contain the *ATG2* promoter (1,240 bp upstream of the start codon), the coding sequence for Atg2-3×HA-EGFP, and the *ATG2* terminator (680 bp downstream of the stop codon). Plasmids for overexpression of Atg2-EGFP or Atg18 were constructed as follows. The *ATG2-EGFP* and *ATG18* genes were amplified by PCR from genomic DNA from a yeast strain in which the genomic *ATG2* gene was tagged with EGFP by a PCR-based method. The resultant PCR products were cloned into p426GPD or p424GPD (3). The HRV3C protease recognition sequence and the His-tag sequence were inserted into p426GPD-*ATG2-EGFP* and p424GPD-*ATG18* using the PrimeSTAR Mutagenesis Basal Kit (TaKaRa). The Protein A tag was amplified by PCR from pYM13 (1) using the primer containing the HRV3C protease recognition sequence. This fragment was inserted into p424GPD-ATG18. Plasmids expressing Atg2 variants, including truncated mutants, amino-acid substitution mutants, fusions with the amphipathic helix of *H. sapiens* Nup133 were constructed using the PrimeSTAR Mutagenesis Basal Kit. Plasmids expressing Atg2 mutants fused with the amphipathic helix of *S. cerevisiae* Gcs1 or the

transmembrane domain of Sec71 were constructed using the In-Fusion Kit (Clontech). The plasmid pGEX6P1-GFP-Nanobody was a gift from Dr. Kazuhisa Nakayama (Addgene plasmid # 61838) (4).

Media

For fluorescence microscopy, yeast cells were cultured at 30°C in SD+CA+ATU medium [0.17% yeast nitrogen base without amino acids and ammonium sulfate (YNB w/o aa and as), 0.5% ammonium sulfate, 0.5% casamino acids, and 2% glucose supplemented with 0.002% adenine sulfate, 0.002% tryptophan, and 0.002% uracil]. When cells carried plasmids derived from pRS316, pRS416, or p426GPD, SD+CA+AT (SD+CA+ATU without uracil) was used, whereas when cells carried plasmids derived from p424GPD and p426GPD, SD+CA+A (SD+CA+ATU without uracil and tryptophan) was used. To induce autophagy, cells were treated with 0.2 μg/ml rapamycin or incubated in nitrogen starvation medium (SD-N; 0.17% YNB w/o aa and as and 2% glucose).

Immunoblotting

Yeast cells pellets were treated with 20% trichloroacetic acid on ice for 15 min, and then centrifuged at 15,000 *g* for 5 min. The pellets were washed with ice-cold acetone, dried at room temperature, and suspended in SDS sample buffer [100 mM Tris-HCl (pH 7.5), 2% SDS, 20 mM dithiothreitol (DTT), 10% glycerol, and a trace amount of bromophenol blue] by mixing at 65°C for 10 min. The cells were disrupted using FastPrep-24 (MP Biomedicals) and 0.5-mm YZB zirconia beads (Yasui Kikai). These samples were boiled for 3 min and centrifuged at 15,000 *g* for 1 min. The supernatants were subjected to immunoblotting analysis with antibodies

against GFP (11814460001; Roche), HA (3F10; Roche), and Ape1 (anti-API-2; our laboratory stocks).

ALP Assay

To quantitatively examine autophagic activities, alkaline phosphatase (ALP) activities of Pho8Δ60 in cell lysates were measured as described previously (5).

Immunoprecipitation

GFP-nanobody (GFP-binding protein)-conjugated magnetic beads (GBP beads) were prepared according to the manufacture's protocol. In brief, NHS FG beads (Tamagawa Seiki) were treated with methanol, and then incubated with GFP-nanobody at room temperature for 30 min. The magnetic beads were mixed with 1 M 2-aminoethanol (pH 8.0) at 4°C for 16–20 h to quench the conjugation reaction, washed three times with wash buffer [10 mM HEPES-NaOH (pH7.9), 50 mM KCl, 1 mM EDTA, and 10% glycerol], and stored in wash buffer containing 1 mg/ml bovine serum albumin (BSA) (A7030; Sigma-Aldrich).

Yeast cells were disrupted in IP buffer [50 mM Tris-HCl (pH 8.0), 150 mM NaCl, 10% glycerol, 1 mM EDTA, 1 mM EGTA, and 50 mM NaF] containing 2× Complete protease inhibitor cocktail (Roche) using a Multi-beads Shocker (Yasui Kikai) and 0.5-mm YZB zirconia beads, and then treated with 0.1% CHAPS by rotating test tubes at 4°C for 30 min. The lysates were cleared by successive centrifugations at 15,000 *g* for 10 min and 30 min. The supernatants were mixed with GBP beads at 4°C for 2 h. The beads were washed three times with IP buffer containing 0.1% CHAPS, and bound proteins were eluted by boiling the beads in SDS sample buffer for 3 min. The samples were subjected to immunoblotting analysis using antibodies

against HA (3F10; Roche), Atg9 (anti-Apg9p-N15; our laboratory stocks) and Atg18 (anti-18-2; our laboratory stocks).

Fluorescence Microscopy

Fluorescence microscopy to determine the PAS localization of Atg2-HA-GFP was performed on an inverted fluorescence microscope (IX83; Olympus) equipped with an electron-multiplying CCD camera (ImagEM C9100-13; Hamamatsu Photonics), and a 150× objective lens (UAPON 150XOTIRF, NA/1.45; Olympus). A 488-nm blue laser (50 mW; Coherent) and a 588-nm yellow laser (50 mW; Coherent) were used for excitation of GFP and mCherry, respectively. Fluorescence was filtered with a dichroic mirror reflecting 405-nm, 488-nm, and 588-nm wavelengths (Olympus) and separated into two channels using the DV2 multichannel imaging system (Photometrics) equipped with a Di02-R594-25x36 dichroic mirror (Semrock). Fluorescence was further filtered with a TRF59001-EM ET bandpass filter (Chroma) for the GFP channel and an FF01-624/40-25 bandpass filter (Semrock) for the mCherry channel. Images were acquired using MetaMorph software (Molecular Devices) and processed using Fiji (ImageJ) (6, 7).

Fluorescence microscopy of the isolation membrane was performed on a DeltaVision Elite (GE Healthcare) microscope system equipped with a scientific CMOS camera (pco.edge 5.5; PCO AG) and a 60× objective lens (PLAPON, NA/1.42; Olympus). Twenty-five z-stacks at 0.2 μm intervals were taken and deconvolved using the SoftWoRx software. The perimeter of the isolation membrane was measured using the ImageJ Script described in ImageJ Script S1. Half of the perimeter was regarded as the length of the isolation membrane.

Protein Purification

The yeast strain BJ3505, which lacks the genomic *ATG2* and *ATG18* genes, was used for protein purification. Cells overexpressing Atg2-GFP-His (hexa-histidine tag), Atg18-His, Atg18-Protein A, or both Atg2-GFP-His and Atg18 from multi-copy plasmids were cultured to mid-log phase (OD_{600} = ~2), and then treated with rapamycin for 3 h. To purify Atg2-GFP-His or Atg2-GFP-His complexed with Atg18, cells were disrupted in buffer A [75 mM HEPES-KOH (pH 8.0), 500 mM NaCl, 10% glycerol, 20 mM imidazole, and 3.5 mM β-mercaptoethanol] containing 0.2 mM phenylmethylsulfonyl fluoride (PMSF) and 2× Complete protease inhibitor cocktail (Roche) using a Multi-beads Shocker (Yasui Kikai) and 0.5-mm YZB zirconia beads. Triton X-100 was added to the lysates to a final concentration of 0.2%, and then the lysates were rotated at 4°C for 30 min and cleared by centrifugation at 10,000 *g* for 10 min and 30 min. The resultant supernatants were rotated with Ni-NTA agarose (QIAGEN) at 4°C for 2 h. The resins were washed with buffer B [50 mM HEPES-KOH (pH 8.0), 1 M NH_4Cl, 10% glycerol, 20 mM imidazole, and 3.5 mM β-mercaptoethanol]. Bound proteins were eluted with buffer C [50 mM HEPES-KOH (pH 7.2), 500 mM NaCl, 10% glycerol, 500 mM imidazole, and 3.5 mM β-mercaptoethanol]. Proteins were concentrated using Vivaspin columns (Sartorius) or Microcon concentrators (Millipore), and stored at -80°C.

The Atg18 mutants used in Figs. 4D, S5B and S5D were purified similarly, except for the following modifications. The lysates were solubilized with 1% Triton X-100. Proteins eluted with buffer C were treated with His-tagged HRV 3C protease (Funakoshi) to cleave the recognition sequence between Atg18 and the His tag, and then dialyzed against buffer D [20 mM HEPES-KOH (pH 8.0), 1 M NaCl, 10% glycerol, 20 mM imidazole, and 3.5 mM β-mercaptoethanol]; the resultant solutions were again mixed with Ni-NTA agarose at 4°C for 30 min. The unbound fractions were collected, dialyzed against buffer E [20 mM HEPES-KOH

(pH 8.0), 150 mM NaCl, 10% glycerol, and 7 mM β-mercaptoethanol], concentrated using Vivaspin columns, and stored at -80°C.

To purify Atg18 used in Fig. 4C, cells expressing Atg18–Protein A were disrupted in buffer F [20 mM HEPES-KOH (pH 7.2), 150 mM NaCl, and 10% glycerol] containing 2× Complete protease inhibitor cocktail, and solubilized with 0.2% Triton X-100. These lysates were cleared by centrifugation, and the supernatants were rotated with IgG Sepharose 6 Fast Flow (GE Healthcare) at 4°C for 2 h. The resins were washed with buffer G [20 mM HEPES-KOH (pH 7.2), 1 M NaCl, and 10% glycerol] containing 0.2% Triton X-100. Bound proteins were eluted with buffer F containing 0.2% Triton X-100 and His-tagged HRV 3C protease, which cleaves the recognition sequence between Atg18 and Protein A. Atg18 was further purified by Mono Q HR 5/5 column chromatography (GE Healthcare) using 20 mM HEPES-KOH (pH 7.2) containing 150–400 mM NaCl and 10% glycerol, and then concentrated using Vivaspin columns.

GFP-nanobody (8) used for immunoprecipitation was purified as follows. *E. coli* BL21 cells carrying pGEX6P1-GFP-Nanobody (Addgene) were cultured in LB media (10 mg/ml tryptone, 5 mg/ml yeast extract, and 10 mg/ml NaCl) containing 50 μg/ml ampicillin at 37°C to an OD_{600} of ~0.5, and treated with 0.1 mM isopropyl-β-D-thiogalactopyranoside at 16°C overnight. Cells were harvested and disrupted in buffer H [20 mM HEPES-KOH (pH 7.2), and 150 mM NaCl] containing 2 mM DTT, 1 mM EDTA, and 0.1 mM PMSF by sonication. The lysate was rotated with glutathione–Sepharose 4B resin (GE Healthcare) at 4°C for 45 min. The resin was washed with buffer H, and bound proteins were eluted with buffer H containing 1 mM DTT and PreScission Protease (GE Healthcare). The proteins were concentrated using Vivaspin columns, and further purified by Superdex200 Increase column chromatography (GE

Healthcare) using buffer H. Purified GFP-nanobody was stored at -80°C in buffer H containing 25% glycerol.

Liposome Preparation

To prepare liposomes, 1,2-dioleoyl-sn-glycero-3-phosphoethanolamine (DOPE) (Avanti Polar Lipids), 1-palmitoyl-2-oleoyl- sn-glycero-3-phosphocholine (POPC) (Avanti Polar Lipids), 1,2-dioleoyl-sn-glycero-3-phospho-L-serine (DOPS) (Avanti Polar Lipids), phosphatidylinositol 3-phosphate (PI3P) (Echelon Biosciences), phosphatidylinositol 3, 5-diphosphate ($PI3,5P_2$) (Wako) 1,2-dioleoyl-sn-glycero-3-phosphoethanolamine-N-(lissamine rhodamine B sulfonyl) (DO-Rho-PE) (Avanti Polar Lipids), 1-oleoyl-2-{12-[(7-nitro-2-1,3-benzoxadiazol-4-yl)amino]dodecanoyl}-sn-glycero-3-phosphoethanolamine (NBD-LOPE) (Avanti Polar Lipids), and 1,2-distearoyl-sn-glycero-3-phosphoethanolamine-N-[biotinyl(polyethylene glycol)-2000] (DSPE-PEG(2000) Biotin) (Avanti Polar Lipids) were mixed in various combinations in glass tubes, and the organic solvent was evaporated to develop lipid films. These films were swollen and suspended in liposome buffer (20 mM HEPES-KOH (pH 7.2) and 150 mM KCl) at a total lipid concentration of 1 mM. After several freeze–thaw cycles, homogenously sized liposomes were prepared by extrusion through polycarbonate filters with a pore size of 400 nm or 100 nm. The smallest liposomes used in this study (~50 nm) were prepared by sonicating liposomes after freeze-thaw cycles. The sizes of liposomes were analyzed by dynamic light scattering measurements (Zetasizer Nano S; Malvern Instruments).

Liposome Flotation Assay

Liposomes (10 nmol lipids) and ~0.5 pmol proteins were mixed in 50 μl of flotation buffer [50 mM HEPES-KOH (pH 7.2) and 150 mM NaCl] containing 0.01% BSA (Figs. 4C-E, S5B and C) or that containing 0.01% BSA and 10% OptiPrep (Fig. 4A, 4B and 4F), and the mixture was incubated at 30°C for 15 min (~0.5 pmol Atg2 and ~50 fmol Atg18 mutants were used in Fig. 4C and D). In Fig. 4A and B, the OptiPrep concentration in the mixture was adjusted to 35% by adding 50 μl of flotation buffer containing 60% OptiPrep, overlaid with 1 ml of flotation buffer containing 30% OptiPrep, which was in turn overlaid with 100 μl of flotation buffer without OptiPrep in test tubes. In Figs. 4C–E, S5B and S5C, the mixtures were adjusted to contain 50% OptiPrep, and then overlaid with 600 and 300 μl of flotation buffer containing 30 and 0% OptiPrep, respectively. In Fig. 4F, the mixtures adjusted to contain 35% OptiPrep was overlaid with 400 and 100 μl of flotation buffer containing 30 and 0% OptiPrep, respectively. These samples were centrifuged at 55,000 rpm for 2 h in a S55S rotor (Hitachi Koki). In Figs. 4A–E, S5B and C, the top, middle 1, middle 2, and bottom fractions (300 μl each) were collected from the top using a micropipette. In Fig. 4F, the top, middle, and bottom fractions (200 μl each) were collected. These fractions were subjected to immunoblotting analysis using antibodies against Atg2 (anti-Atg2p; our laboratory stocks) and Atg18 (anti-18-2; our laboratory stocks).

Liposome Tethering Assay

Liposome tethering assay was performed as described previously (9). Two different liposomes with the following lipid compositions were prepared by sonication: NBD-liposomes (74.0 mol% POPC, 19.7 mol% DOPE, 5.0 mol% PI3P, 1.0 mol% NBD-LOPE, and 0.4 mol% DSPE-PEG(2000)-Biotin) and Rho-liposomes (74.3 mol% POPC, 19.8 mol% DOPE, 5.0 mol% DOPS and 1.0 mol% DO-Rho-PE). NBD-liposomes (3 nmol lipids), Rho-liposomes (1 nmol lipids) and proteins (~1 pmol) were mixed in 50 μl of flotation buffer containing 0.01% BSA

and 10% OptiPrep. The mixture was incubated at 30°C for 15 min, and then mixed with Streptavidin MagneSphere (Promega) and stayed on ice for 10 min. The beads were washed three times with flotation buffer containing 0.01% BSA and 10% OptiPrep, and bound lipids were extracted by methanol, followed by fluorescence spectrophotometry. Rhodamine fluorescence (Ex/Em = 550/570 nm) was normalized with NBD fluorescence (Ex/Em = 465/535 nm).

Table S1. Yeast strains used in this study

Name	Genotype	(Ref.)/Figures
BY4741	*MATa his3Δ1 leu2Δ0 met15Δ0 ura3Δ0*	(10)
ScTK284	BY4741 *atg2Δ::natNT2*	2B, S1D, S3A, S4B, S4E
ScTK296	BY4741 *ATG17-2×mCherry::hphNT1 atg2Δ::natNT2*	3D, S4G
ScTK297	BY4741 *pho8::kanMX4- P_{GPD}-pho8Δ60 atg2Δ::natNT2*	S2
ScTK298	BY4741 *his3*::pRS303-*PGK1-EGFP atg2Δ::natNT2*	1A, 2E, 3A, 3E, S1C, S3C, S4A, S4D, S4I
ScTK467	BY4741 *ATG17-2×mCherry::hphNT atg2Δ::natNT2 atg8Δ::kanMX4*	2D, S3B, S4F
ScTK483	ScTK467 *his3*::pRS303-*ATG2-3×HA-EGFP*	1B, 2C, 3B
ScTK484	ScTK467 *his3*::pRS303-*$atg2^{\Delta 2\text{-}21}$-3×HA-EGFP*	3B
ScTK485	ScTK467 *his3*::pRS303-*$ATG2^{\Delta 1374\text{-}1592}$-3×HA-EGFP*	1B
ScTK486	ScTK467 *his3*::pRS303-*$atg2^{\Delta 1347\text{-}1592}$-3×HA-EGFP*	1B
ScTK487	ScTK467 *his3*::pRS303-*$atg2^{F1352D\ I1355D}$-3×HA-EGFP*	2C
ScTK489	ScTK467 *his3*::pRS303-*$atg2^{\Delta 2\text{-}12}$-3×HA-EGFP*	3B
ScTK490	ScTK467 *his3*::pRS303-*$atg2^{F1352D}$-3×HA-EGFP*	2C
W303-1a	*MATa ade2-1 ura3-1 his3-11,15 trp1-1 leu2-3,112 can1-100*	(11)
ScTK768	W303-1A, *ade2::ADE2 leu2::2×mCherry-ATG8-hphNT1 kanMX4*::*P_{GPD}-APE1 trp1-1*::pRS304-*P_{GPD}-APE1 atg2Δ::natNT2*	-
ScTK772	ScTK768 *his3*::pRS303-*ATG2-3×HA-EGFP*	3C
ScTK773	ScTK768 *his3*::pRS303-*$atg2^{\Delta 2\text{-}12}$-3×HA-EGFP*	3C
ScTK774	ScTK768 *his3*::pRS303-*$atg2^{\Delta 2\text{-}21}$-3×HA-EGFP*	3C
BJ3505	*MATa pep4::HIS3 prb1-Δ1.6R 1ys2-208 trp1-Δ101 ura3-52 gal2 can*	(12)
ScTK48	BJ3505 *atg18Δ::zeoNT3 atg2Δ::natNT2*	4, S4H

Table S2. Plasmids used in this study

Name	Description	(Ref.)/Figures
-	pRS316-*ATG2-3×HA-EGFP*	(lab stock)/1A, 2B, 2E, 3A, 3E, S1C, S1D, S2, S3A, S3C, S4A, S4B, S4D-F, S4H, S4I
pTKO2	pRS316-*atg2$^{\Delta 2\text{-}12}$-3×HA-EGFP*	3A, S2D, S4A, S4B
pTKO3	pRS316-*atg2$^{\Delta 2\text{-}21}$-3×HA-EGFP*	3A, 3E, S2D, S2F, S4A, S4B, S4I
pTKO4	pRS316-*atg2$^{\Delta 2\text{-}28}$-3×HA-EGFP*	3A, S2D, S4A, S4B
pTKO5	pRS316-*atg2$^{\Delta 2\text{-}46}$-3×HA-EGFP*	3A, S2D, S4A, S4B
pTKO10	pRS316-*ATG2$^{\Delta 1374\text{-}1592}$-3×HA-EGFP*	1A, S1C, S1D, S2A
pTKO12	pRS316-*atg2$^{\Delta 1347\text{-}1592}$-3×HA-EGFP*	1A, 2B, 2D, 2E, S1C, S1D, S2A, S2C, S3B, S3C
pTKO13	pRS316-*atg2$^{\Delta 1305\text{-}1592}$-3×HA-EGFP*	1A, S1C, S1D, S2A
pTKO14	pRS316-*atg2$^{\Delta 1269\text{-}1592}$-3×HA-EGFP*	1A, S1C, S1D, S2A
pTKO38	pRS316-*atg2^{F1352D}-3×HA-EGFP*	2B, S2B, S3A
pTKO39	pRS316-*atg2$^{F1352D\ I1355D}$-3×HA-EGFP*	2B, S2B, S3A
pTKO40	pRS316-*ATG2$^{F1352W\ I1355W}$-3×HA-EGFP*	2B, S2B, S3A
pTKO43	pRS316-*atg2$^{\Delta 1347\text{-}1592}$-ScGCS1^{AH}-3×HA-EGFP*	2E, S2C, S3B, S3C
pTKO44	pRS316-*atg2$^{\Delta 1347\text{-}1592}$-ScGCS1$^{AH\ TM}$-3×HA-EGFP*	2E, S2C, S3B, S3C
pTKO45	pRS316-*atg2$^{\Delta 1347\text{-}1592}$-HsNUP133^{AH}-3×HA-EGFP*	2D, 2E, S2C, S3C
pTKO46	pRS316-*atg2$^{\Delta 1347\text{-}1592}$-HsNUP133$^{AH\ I255D}$-3×HA-EGFP*	2D, 2E, S2C, S3C
pTKO78	pRS316-*atg2$^{10\text{-}12D}$-3×HA-EGFP*	S2E, S4D-F
pTKO83	pRS416-*P$_{GPD}$-atg2$^{1\text{-}46}$-3×HA-EGFP*	S4G
pTKO118	pRS416-*P$_{GPD}$-atg2$^{1\text{-}46\ 10\text{-}12D}$-3×HA-EGFP*	S4G
pTKO74	pRS316-*Sec71TMD-atg2$^{\Delta 2\text{-}21}$-3×HA-EGFP*	3D,3E, S2F, S4H, S4I
pTKO133	p426GPD-*ATG2-EGFP-HRV3Csite-His$_6$*	4A-G, S5A, S5C-E
pTKO136	p426GPD-*atg2$^{\Delta 1347\text{-}1592}$-EGFP-HRV3Csite-His$_6$*	4B, 4E-G, S5A, S5E
pTKO137	p426GPD-*atg2$^{F1352D\ I1355D}$-EGFP-HRV3Csite-His$_6$*	4E, S5A
pTKO144	p426GPD-*atg2$^{\Delta 2\text{-}21}$-EGFP-HRV3Csite-His$_6$*	4B, 4E, 4G, S5A, S5E
pTKO146	p426GPD-*atg2$^{\Delta 2\text{-}21\ \Delta 1347\text{-}1592}$-EGFP-HRV3Csite-His$_6$*	4B, 4G, S5A
pTKO228	p426GPD-*atg2$^{\Delta 1347\text{-}1592}$-HsNUP133^{AH}-EGFP-HRV3Csite-His$_6$*	4F, S5A
pTKO121	p424GPD-*ATG18*	4E, 4F, S5A, S5C, S5E
pTKO122	p424GPD-*ATG18-HRV3Csite-His$_6$*	4D, S5A, S5B, S5D

pTKO123	p424GPD-*ATG18-HRV3Csite-ProtA*	4C, S5A
pTKO126	p424GPD-*atg18*$^{P72A\ R73A}$*-HRV3Csite-His*$_6$	4D, S5A, S5B, S5D
pTKO129	p424GPD-*atg18*$^{R285T\ R286T}$*-HRV3Csite-His*$_6$	4D, S5A, S5B, S5D
-	pGEX6P1-GFP-Nanobody	(4)

ImageJ Script S1

```
rename("Atg8");

//maximum intensity projection
run("Z Project...", "projection=[Max Intensity]");
run("Split Channels");
close();
selectWindow("C1-MAX_Atg8");

//find the isolation membranes
setAutoThreshold("Moments dark");
run("Convert to Mask");
run("Analyze Particles...", "size=0.1-Infinity add in_situ");

//Measure the perimeter of the isolation membrane
roiManager("Measure");

roiManager("Deselect");
roiManager("Delete");
selectWindow("C1-MAX_Atg8");
close();
selectWindow("Atg8");
close();
```

SI References

1. Janke C, et al. (2004) A versatile toolbox for PCR-based tagging of yeast genes: New fluorescent proteins, more markers and promoter substitution cassettes. *Yeast* 21(11):947–962.
2. Sikorski RS, Hieter P (1989) A system of shuttle vectors and yeast host strains designed for efficient manipulation of DNA in *Saccharomyces cerevisiae*. *Genetics* 122(1):19–27.
3. Mumberg D, Müller R, Funk M (1995) Yeast vectors for the controlled expression of heterologous proteins in different genetic backgrounds. *Gene* 156(1):119–22.
4. Katoh Y, Nozaki S, Hartanto D, Miyano R, Nakayama K (2015) Architectures of multisubunit complexes revealed by a visible immunoprecipitation assay using fluorescent fusion proteins. *J Cell Sci* 128(12):2351–62.
5. Noda T, Matsuura A, Wada Y, Ohsumi Y (1995) Novel system for monitoring autophagy in the yeast *Saccharomyces cerevisiae*. *Biochem Biophys Res Commun* 210(1):126–132.
6. Schneider CA, Rasband WS, Eliceiri KW (2012) NIH Image to ImageJ: 25 years of image analysis. *Nat Methods* 9(7):671–675.
7. Schindelin J, et al. (2012) Fiji: An open-source platform for biological-image analysis. *Nat Methods* 9(7):676–682.
8. Rothbauer U, et al. (2006) Targeting and tracing antigens in live cells with fluorescent nanobodies. *Nat Methods* 3(11):887–889.
9. Ragusa MJ, Stanley RE, Hurley JH (2012) Architecture of the Atg17 complex as a scaffold for autophagosome biogenesis. *Cell* 151(7):1501–1512.
10. Brachmann CB, et al. (1998) Designer deletion strains derived from *Saccharomyces cerevisiae* S288C: A useful set of strains and plasmids for PCR-mediated gene

disruption and other applications. *Yeast* 14(2):115–132.

11. Thomas BJ, Rothstein R (1989) Elevated recombination rates in transcriptionally active DNA. *Cell* 56(4):619–30.
12. Jones EW, Zubenko GS, Parker RR (1982) *PEP4* gene function is required for expression of several vacuolar hydrolases in *Saccharomyces cerevisiae*. *Genetics* 102(4):665–77.
13. Ashkenazy H, Erez E, Martz E, Pupko T, Ben-Tal N (2010) ConSurf 2010: Calculating evolutionary conservation in sequence and structure of proteins and nucleic acids. *Nucleic Acids Res* 38(SUPPL. 2):529–533.
14. Fischer JD, Mayer CE, Söding J (2008) Prediction of protein functional residues from sequence by probability density estimation. *Bioinformatics* 24(5):613–620.
15. Tamura N, et al. (2017) Differential requirement for ATG2A domains for localization to autophagic membranes and lipid droplets. *FEBS Lett* 591(23):3819–3830.

Figure legends

Fig. S1. Supplemental data related to Fig. 1. (A) Analysis of amino acid conservation of Atg2 by ConSurf (13). Conserved amino acid residues are enriched in both the N- and C-terminal regions. (B) Schematic diagram of C-terminally truncated mutants of Atg2. The amphipathic α-helix required for autophagy is colored red. (C) Yeast cells were grown to mid-log phase, treated with rapamycin, and examined by immunoblotting using anti-GFP antibodies. GFP', GFP fragments generated by vacuolar degradation of Pgk1-GFP. (D) Cells were treated with rapamycin for 1 h, and subjected to immunoprecipitation analysis using GFP-nanobody. Total cell lysates (input) and immunoprecipitates (IP) were analyzed by immunoblotting using anti-HA, anti-Atg18, and anti-Atg9 antibodies.

Fig. S2. ALP activities in yeast cells expressing the Atg2 mutants. Yeast cells expressing Pho8Δ60 and the Atg2 mutants were grown to mid-log phase, and then incubated in nitrogen-starvation medium for 4 h, and ALP activities in these cells were measured. Error bars, standard deviations (n = 3). AU, arbitrary unit. (A) C-terminal deletion mutants. (B) Amphipathic helix mutants. (C) Δ1347-1592 mutants fused with the amphipathic helix of ScGcs1 or HsNup133. (D) N-terminal deletion mutants. (E) $Atg2^{10\text{-}12D}$ mutant. (F) $Sec71^{TMD}$-$Atg2^{\Delta 2\text{-}21}$ mutant.

Fig. S3. Supplemental data related to Fig. 2. (A) Interactions of the Atg2 mutants for F1352 and I1355 with Atg18 and Atg9 were examined as described in Fig. S1D. (B) The PAS localization of the Atg2-HA-GFP mutants was examined as described in Fig. 1B. Scale bar, 5 μm. Error bars, standard deviations (n = 3). The results for $Atg2^{\Delta 1347\text{-}1592}$ are the same as those presented in Fig. 2D. (C) The cleavage of Pgk1-GFP in the Atg2 mutants were examined as described in Fig.

S1C.

Fig. S4. Supplemental data related to Fig. 3. (A) Pgk1-GFP cleavage in the N-terminal deletion mutants of Atg2 were analyzed as described in Fig. S1C. (B) Co-immunoprecipitation analysis was performed as described in Fig. S1D. (C) Analysis of amino acid conservation in the N-terminal region of Atg2, performed using FRpred (14). In the $Atg2^{10\text{-}12D}$ mutant, residues Q10-K11-R12 were replaced with aspartic acid. (D) Cells were treated with rapamycin and examined for Ape1 maturation and Pgk1-GFP cleavage as described in Fig. 1A and S1C. (E) The interactions of $Atg2^{10\text{-}12D}$ with Atg18 and Atg9 were examined as described in Fig. S1D. (F) The PAS localization of $Atg2^{10\text{-}12D}$ was analyzed as described in Fig. 1B. Scale bar, 5 μm. (G) The Atg2 mutants were overexpressed in yeast cells, and their localization under normal conditions was analyzed by fluorescence microscopy. Scale bar, 5 μm. (H) Cell fractionation analysis of the Atg2 mutants used in Fig. 3. *atg2*Δ cells expressing Atg2-HA-GFP or $Sec71^{TMD}$-$Atg2^{\Delta 2\text{-}21}$-HA-GFP were converted to spheroplasts, treated with rapamycin for 1 h, and then ruptured by filtration in buffer I [20 m HEPES-KOH (pH 7.2), 150 mM NaCl, 0.5 M sorbitol, 5 mM EDTA] containing 2× Complete protease inhibitor cocktail and 2 mM Pefabloc (Roche). Lysates were cleared by centrifugation at 1,000 *g* for 5 min (total), and centrifuged at 15,000 *g* for 30 min to obtain pellets (P15) and supernatants. The supernatants were centrifuged at 100,000 *g* for 1 h, and the pellets (P100) and supernatants (S100) were analyzed by immunoblotting using antibodies against HA and Dpm1 (5C5; Invitrogen) (I) Cells were treated with rapamycin for 4 h and examined for Pgk1-GFP cleavage as described in Fig. S1C.

Fig. S5. Supplemental data related to Fig. 4. (A) Coomassie-stained gel images for SDS-PAGE of purified Atg2-GFP-His, Atg2-GFP-His complexed with Atg18, and Atg18 used in Fig. 4 and

S5. (B) Flotation assay with the Atg18 mutants and liposomes containing PI(3,5)P_2. (C) Flotation assay with the Atg2–Atg18 complex and liposomes without PI3P. (D) *In vitro* binding assay for the interaction between Atg2 and the Atg18 mutants. Atg2-GFP-His and the Atg18 mutants were incubated at 30°C for 25 min in flotation buffer containing 0.01% BSA, and the samples were then mixed with GBP beads at 4°C for 90 min. Bound proteins were eluted by incubating beads in SDS sample buffer at 65°C for 10 min, followed by immunoblotting. (E) Liposome tethering assay with the Atg2-Atg18 complex was performed as described in Fig. 4G.

Fig. S6. Amino-acid alignment of the C-terminal region of Atg2, encompassing the amphipathic helix. Alignment of *S. cerevisiae* Atg2, *Schizosaccharomyces pombe* Atg2, and *H. sapiens* Atg2A was generated using Clustal Omega. The sequences identified as amphipathic helices in this paper or by Tamura et al (15) are boxed in red.

Figure S1


A
1
500
1000
1500
The conservation scale:
1 2 3 4 5 6 7 8 9
Variable
Average
Conserved


B
1
1592
WT
Δ1374-1592
Δ1347-1592
Δ1305-1592
Δ1269-1592

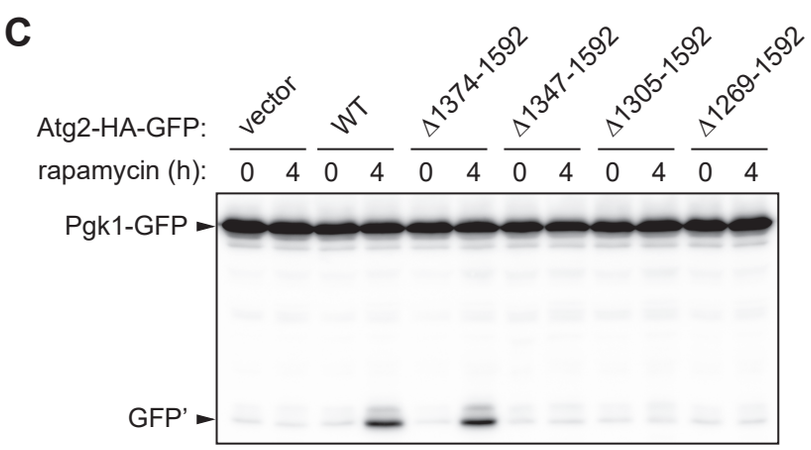
C
Atg2-HA-GFP:
vector
WT
Δ1374-1592
Δ1347-1592
Δ1305-1592
Δ1269-1592
rapamycin (h):
0 4 0 4 0 4 0 4 0 4 0 4
Pgk1-GFP
GFP'

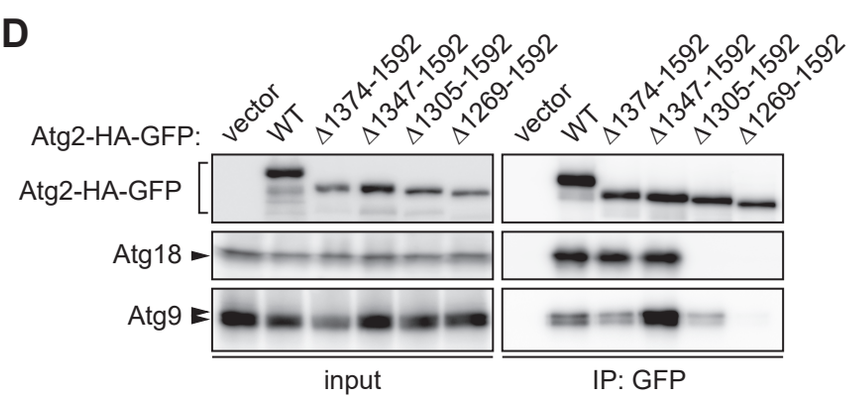
D
Atg2-HA-GFP:
vector
WT
Δ1374-1592
Δ1347-1592
Δ1305-1592
Δ1269-1592
vector
WT
Δ1374-1592
Δ1347-1592
Δ1305-1592
Δ1269-1592
Atg2-HA-GFP
Atg18
Atg9
input
IP: GFP

Figure S2

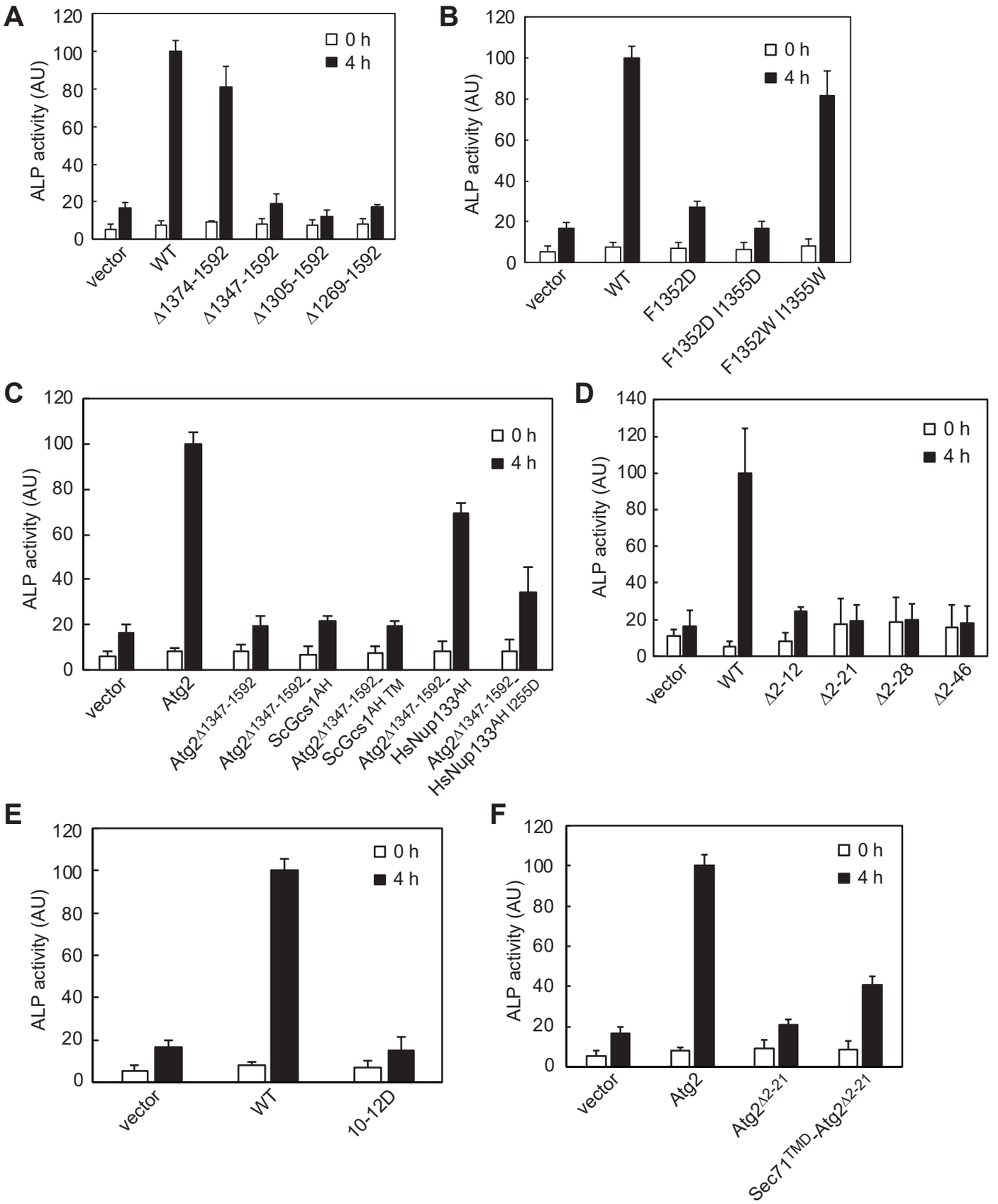
A
ALP activity (AU)
0 h
4 h
vector
WT
Δ1374-1592
Δ1347-1592
Δ1305-1592
Δ1269-1592
B
ALP activity (AU)
0 h
4 h
vector
WT
F1352D
F1352D I1355D
F1352W I1355W
C
ALP activity (AU)
0 h
4 h
vector
Atg2
Atg2Δ1347-1592
Atg2Δ1347-1592-ScGcs1AH
Atg2Δ1347-1592-ScGcs1AH TM
Atg2Δ1347-1592-HsNup133AH
Atg2Δ1347-1592-HsNup133AH I255D
D
ALP activity (AU)
0 h
4 h
vector
WT
Δ2-12
Δ2-21
Δ2-28
Δ2-46
E
ALP activity (AU)
0 h
4 h
vector
WT
10-12D
F
ALP activity (AU)
0 h
4 h
vector
Atg2
Atg2Δ2-21
Sec71TMD-Atg2Δ2-21

Figure S3

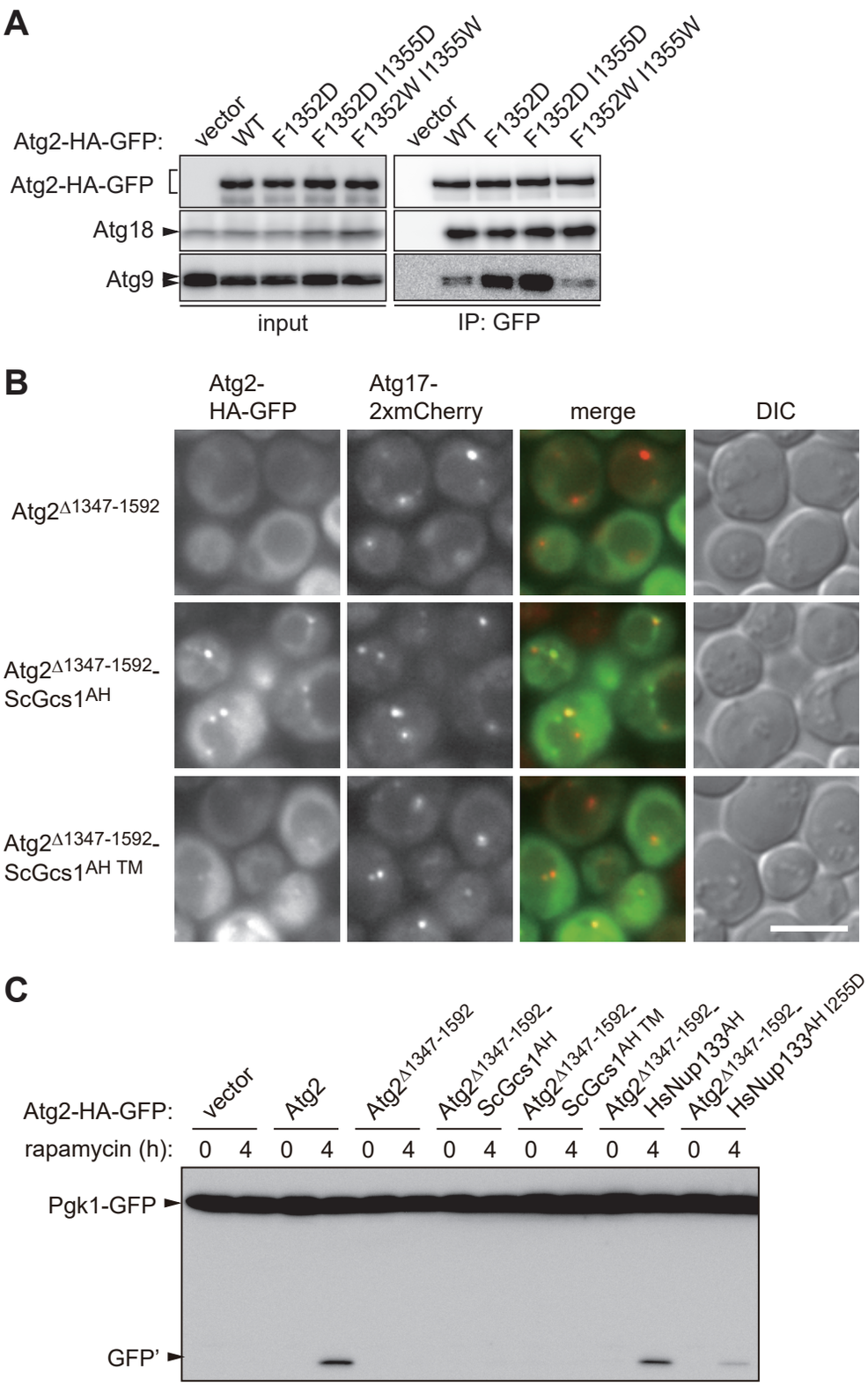
A
Atg2-HA-GFP:
vector
WT
F1352D
F1352D I1355D
F1352W I1355W
vector
WT
F1352D
F1352D I1355D
F1352W I1355W
Atg2-HA-GFP
Atg18
Atg9
input
IP: GFP
B
Atg2-HA-GFP
Atg17-2xmCherry
merge
DIC
Atg2Δ1347-1592
Atg2Δ1347-1592-ScGcs1AH
Atg2Δ1347-1592-ScGcs1AH TM
C
Atg2-HA-GFP:
vector
Atg2
Atg2Δ1347-1592
Atg2Δ1347-1592-ScGcs1AH
Atg2Δ1347-1592-ScGcs1AH TM
Atg2Δ1347-1592-HsNup133AH
Atg2Δ1347-1592-HsNup133AH I255D
rapamycin (h):
0 4 0 4 0 4 0 4 0 4 0 4 0 4
Pgk1-GFP
GFP'

Figure S4

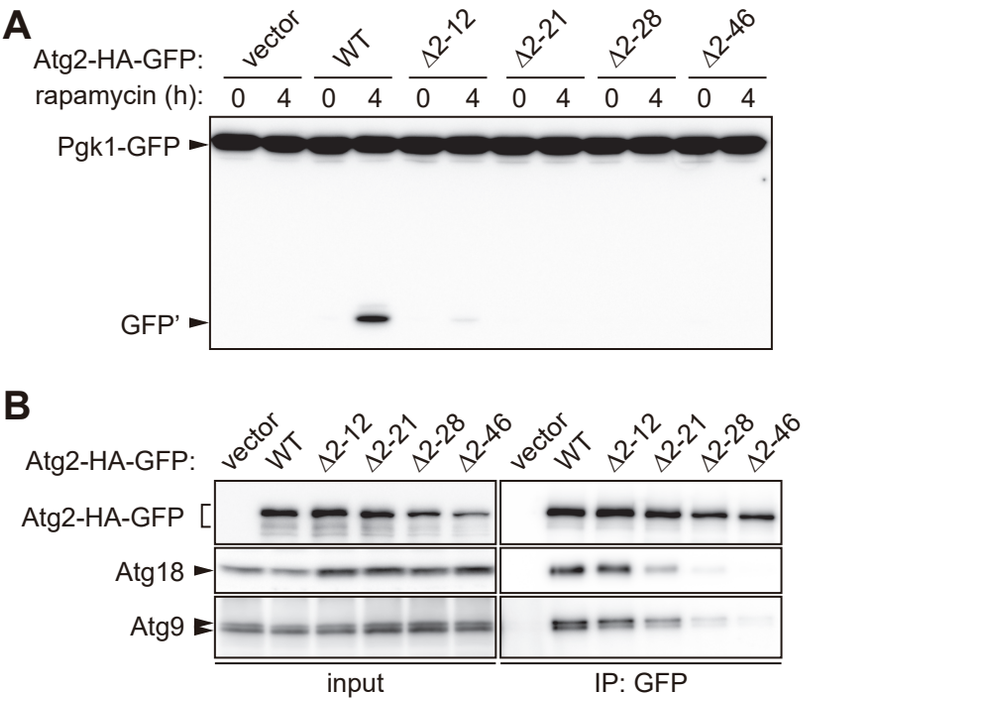
A
Atg2-HA-GFP:
vector
WT
Δ2-12
Δ2-21
Δ2-28
Δ2-46
rapamycin (h):
0 4 0 4 0 4 0 4 0 4 0 4
Pgk1-GFP
GFP'
B
Atg2-HA-GFP:
vector
WT
Δ2-12
Δ2-21
Δ2-28
Δ2-46
Atg2-HA-GFP
Atg18
Atg9
input
IP: GFP
C
1
46
WT MAFWLPQNIQKRLLLYVLQQISLFSNIDLSNLDVSIGSKSHFSFHD
10-12D MAFWLPQNIDDDLLLYVLQQISLFSNIDLSNLDVSIGSKSHFSFHD
Conservation: bad 1 2 3 4 5 6 7 8 9 good
D
Atg2-HA-GFP:
vector
WT
10-12D
rapamycin (h):
0 4 0 4 0 4
Atg2-HA-GFP
prApe1
mApe1
Pgk1-GFP
GFP'
E
Atg2-HA-GFP:
vector
WT
10-12D
vector
WT
10-12D
Atg2-HA-GFP
Atg18
Atg9
input
IP: GFP

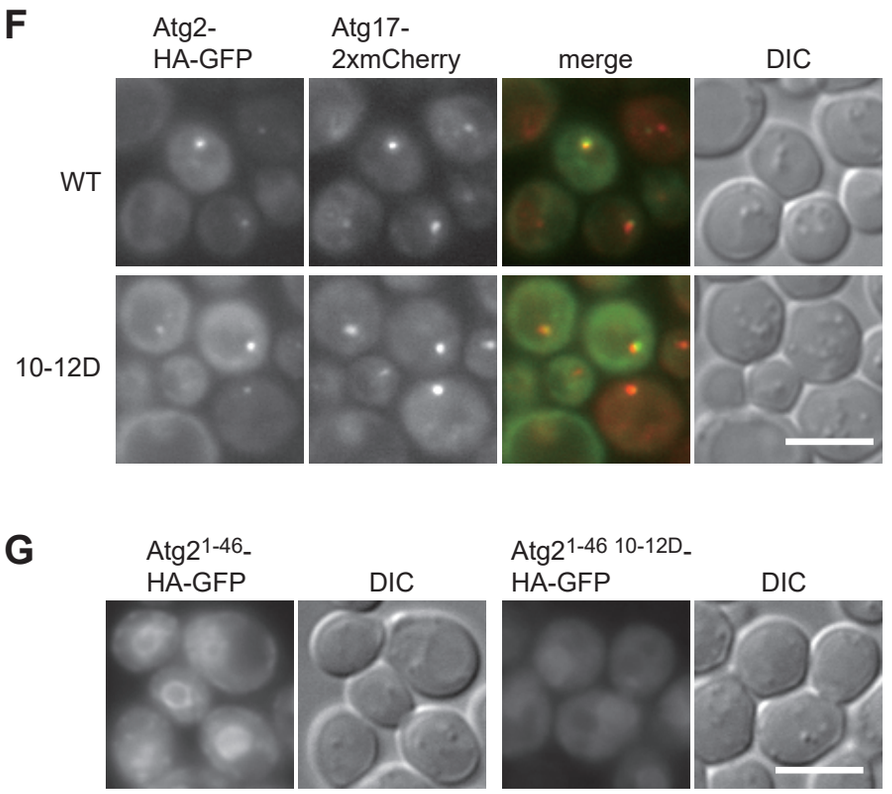
F
Atg2-
HA-GFP
Atg17-
2xmCherry
merge
DIC
WT
10-12D
G
Atg2^1-46-
HA-GFP
DIC
Atg2^1-46 10-12D-
HA-GFP
DIC
H
WT
Sec71^TMD-
Atg2^Δ2-21
total (S1)
P15
P100
S100
total (S1)
P15
P100
S100
Atg2-HA-GFP
Dpm1
I
Atg2-HA-GFP:
vector
Atg2
Atg2^Δ2-21
Sec71^TMD-
Atg2^Δ2-21
rapamycin (h):
0 4 0 4 0 4 0 4
Pgk1-GFP
GFP'

Figure S5

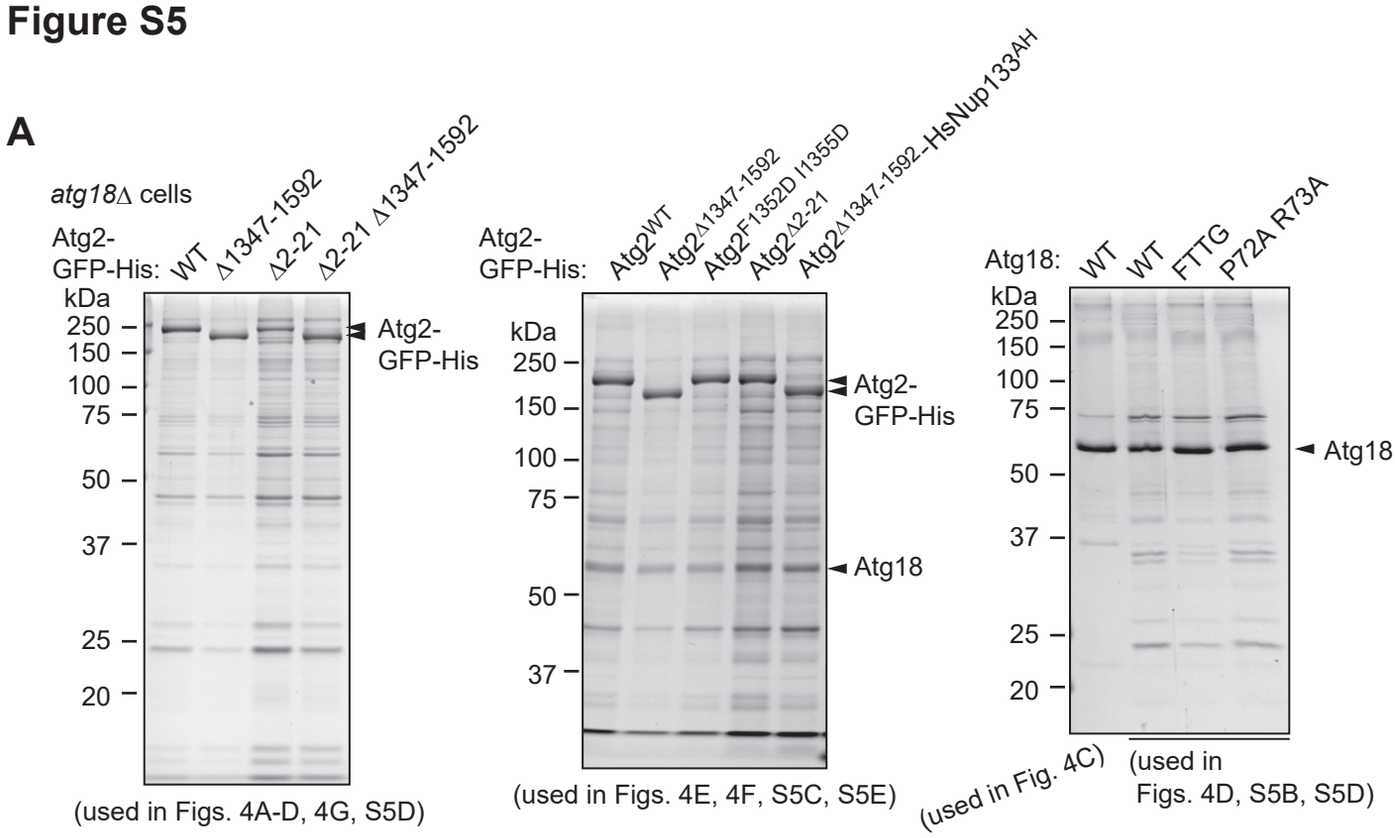

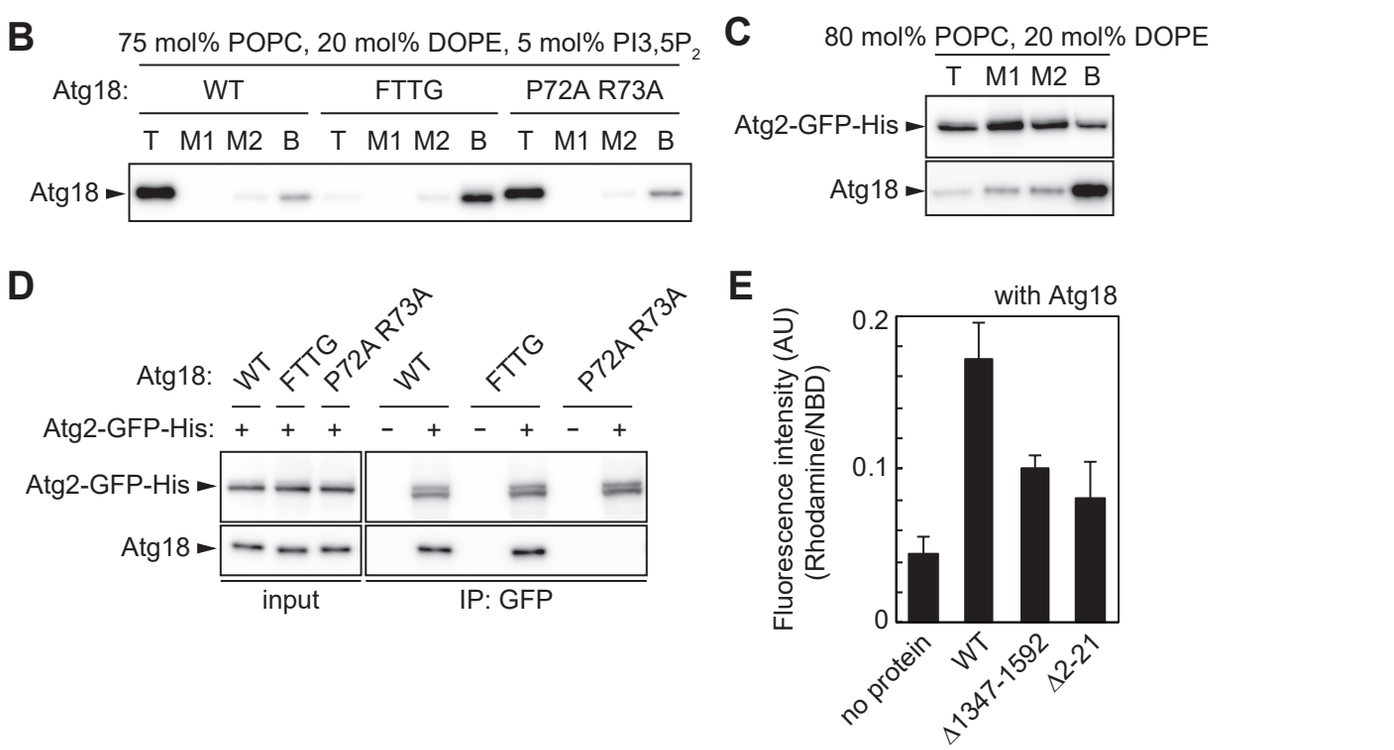

Figure S6